

Chiral tunneling in metallic carbon nanotubes

A. V. Parafilo,^{1,*} I. V. Krive,^{1,2,3} E. N. Bogachek,⁴ U. Landman,⁴ R. I. Shekhter,² and M. Jonson^{2,5,6}
¹*B. Verkin Institute for Low Temperature Physics and Engineering of the National Academy of Sciences of Ukraine, 47 Lenin Avenue, Kharkov 61103, Ukraine*

²*Department of Physics, University of Gothenburg, SE-412 96 Göteborg, Sweden*

³*Physics Department, V. N. Karazin National University, Kharkov 61077, Ukraine*

⁴*School of Physics, Georgia Institute of Technology, Atlanta, Georgia 30332-0430, USA*

⁵*SUPA, Department of Physics, Heriot-Watt University, Edinburgh EH14 4AS, Scotland*

⁶*Division of Quantum Phases and Devices, School of Physics, Konkuk University, Seoul 143-701, Korea*

(Received 14 December 2010; published 31 January 2011)

The concept of chiral tunneling in metallic single-wall carbon nanotubes, originating from the interplay of local electrostatic and pseudomagnetic potentials, is considered and applied to an evaluation of the Josephson current in a nanotube-based superconductor–normal metal–superconductor (SNS) junction and the persistent current in a circular nanotube. In the former case, an oscillatory dependence of the critical supercurrent on the potential strength and the nanotube chiral angle is predicted. In the latter case, the existence of a spontaneous persistent current in an isolated ringlike nanotube is discussed.

DOI: [10.1103/PhysRevB.83.045427](https://doi.org/10.1103/PhysRevB.83.045427)

PACS number(s): 72.10.–d, 74.50.+r

I. INTRODUCTION

Tunneling of nonrelativistic and relativistic fermions through a potential barrier is drastically different. While for nonrelativistic electrons the transmission probability, as a rule, is small and exponentially dependent on the potential strength, massless Dirac fermions freely penetrate potential barriers of arbitrary strength with a probability $D = 1$ for normal incidence (the Klein paradox).¹ The absence of backscattering is explained by the conservation of fermion helicity, i.e., the additional quantum number for relativistic particles with spin. Finite backscattering ($D < 1$) appears in tunneling of massless particles through a scalar (electrostatic) barrier for angles of incidence other than normal or in the presence of a vector potential (“magnetic” scattering).

In metallic single-wall carbon nanotubes (SWNTs), electron transport is known to be ballistic (see, e.g., Ref. 2) and the charged quasiparticles are one-dimensional (1D) Dirac-like massless excitations. Their weak scattering from long-range tube defects is used to explain (by analogy with the Klein paradox) the delocalization of electrons, even in long metallic nanotubes.² Short-range defects cause electron backscattering ($\Delta q \simeq 2k_F$), which for Dirac quasiparticles in SWNTs is described as strong intervalley ($\pm k_F$) transitions. Since particles in different valleys are characterized by opposite helicities, the chiral properties of an individual electron do not play a significant role for electron transport in metallic nanotubes with short-range impurities. Therefore, electron tunneling through such defects in nanotubes is qualitatively the same as for nonrelativistic particles.

We show that a particular type of electron scattering, namely, “chiral tunneling,” can occur in metallic SWNTs as a result of the interplay between long-range (“smooth”) electrostatic and pseudomagnetic potentials. The electrostatic potential (V_d) models ordinary electron scattering by charged impurities (or by nonuniform gate potentials), while the pseudomagnetic potential (V_o) describes the effective vector potential caused by deformations of the nanotube.³ Therefore, we physically study the influence of local strain on electron transport in SWNTs. Chiral tunneling bridges be-

tween ordinary tunneling ($D \ll 1$), which reappears in the limit $V_o \gg V_d$, and Klein tunneling ($D = 1$), which is reached in the opposite limit $V_d \gg V_o$. Chiral tunneling is pronounced when $V_o \simeq V_d$ and is characterized by an oscillatory dependence of the electron transmission coefficient on the chiral phase $\phi_c = U_0 \cos \tilde{\theta}$, where U_0 is the dimensionless potential strength and $\tilde{\theta}$ is an effective chiral angle determined by the nanotube chiral angle and the phase of the pseudomagnetic potential.

We study the effects of chiral tunneling on (i) the Josephson current through nanotube-based superconductor–normal metal–superconductor (SNS) junctions and (ii) the persistent current⁴ in circular nanotubes. As we show here, the critical supercurrent in the first case is an oscillating function of the potential strength and, for special quantized values of the chiral phase ($\phi_c = \pi N$, with N an integer), the resulting supercurrent coincides with that through a fully transparent SNS constriction. In the second case, we find that the persistent current is strongly influenced by the chiral phase. We focus on the interesting problem pertaining to the existence of a spontaneous persistent current (at zero magnetic flux) in an isolated ringlike nanotube with an odd number of electrons. We show that the amplitude of the spontaneous current (caused by a nonsymmetric population of Dirac points) is determined only by the effective chiral angle $\tilde{\theta}$.

II. MODEL

In this paper, we will only consider intravalley electron scattering. Hence we can model the metallic SWNT by the Hamiltonian⁵

$$H_{\pm} = \pm \hbar v_F \begin{pmatrix} 0 & \exp(\pm i\theta) \hat{p}_x \\ \exp(\mp i\theta) \hat{p}_x & 0 \end{pmatrix}, \quad (1)$$

where $j = \pm$ is the valley index, v_F is the Fermi velocity, $\hat{p}_x = -i \partial_x$, θ is the chiral angle of the nanotube ($0 \leq \theta \leq \pi/6$), and the x axis is directed along the cylinder axis.⁶ We shall neglect some small modifications on the electron dispersion induced

by the finite curvature of the nanotube walls⁷ but will comment on their effect at the end.

We first evaluate the transmission coefficient $D(\theta)$ for electron scattering by a “local” chiral potential in a SWNT. Note that the electrostatic (scalar) potential is diagonal in the pseudospin indices and, therefore, unable to induce electron backscattering due to the conservation of helicity for massless Dirac particles. To get nontrivial scattering of chiral particles, we consider, therefore, the phenomenological matrix potential

$$\hat{V}_{\pm}(x) = \begin{pmatrix} V_d(x) & V_o(x) \exp(\pm i\alpha) \\ V_o(x) \exp(\mp i\alpha) & V_d(x) \end{pmatrix}, \quad (2)$$

which mixes the two sublattice components of the electron wave function. The off-diagonal components $V_o(x)$ correspond to “pseudomagnetic effects.”⁸ By using “strain engineering”⁹ of the SWNT (possibly with the help of an atomic force microscope), both V_o and α can be considered as controllable parameters. In particular, the phase α is readily expressed through the components of the strain tensor u_{ik} (Ref. 10) $\{\alpha = -2\tilde{\theta} - \arctan[2u_{xy}/(u_{xx} - u_{yy})]\}$. Therefore, the scattering potential [Eq. (2)] can be produced by elastic deformation of the SWNT. It also appears in the problem of electron scattering in carbon nanopeapods,⁵ where the pseudomagnetic potential is induced by the hybridization of fullerene molecular orbitals with conduction electron states in the chiral nanotube.

III. CHIRAL TUNNELING

We will consider the potentials in Eq. (2) as local and model them by rectangular barriers of width a and heights V_o and V_d in the limit $a \rightarrow 0$, $V_o, V_d \rightarrow \infty$, with $V_o a = \text{const}$ and $V_o/V_d = \text{const}$. The resulting scattering problem is solved for the transmission (t) and reflection (r) amplitudes by the standard procedure of matching plane-wave and evanescent solutions of the Dirac equation, yielding

$$t = \frac{\exp(-iV_o a \cos \tilde{\theta} / \hbar v_F) \sqrt{1 - (V_o/V_d)^2 \sin^2 \tilde{\theta}}}{\sqrt{1 - (V_o/V_d)^2 \sin^2 \tilde{\theta}} \cos \kappa + i \sin \kappa}, \quad (3)$$

$$r = -\frac{V_o \sin \tilde{\theta} \sin \kappa}{V_d \sqrt{1 - (V_o/V_d)^2 \sin^2 \tilde{\theta}} \cos \kappa + i \sin \kappa},$$

where $\kappa = (V_o a / \hbar v_F) [(V_d/V_o)^2 - \sin^2 \tilde{\theta}]^{1/2}$ and $\tilde{\theta} = \theta - \alpha$. These amplitudes depend on several unknown parameters. We will focus on the case $V_o \simeq V_d$, where the effects of chiral tunneling are most pronounced. In this case, the transmission and reflection amplitudes, expressed as $t(\tilde{\theta}) = D(\tilde{\theta})^{1/2} \exp[i\delta_f(\tilde{\theta})]$ and $r(\tilde{\theta}) = R(\tilde{\theta})^{1/2} \exp[i\delta_b(\tilde{\theta})]$, where $R(\tilde{\theta}) = 1 - D(\tilde{\theta})$, take the form

$$D(\tilde{\theta}) = \frac{\cos^2 \tilde{\theta}}{\cos^2(U_0 \cos \tilde{\theta}) \cos^2 \tilde{\theta} + \sin^2(U_0 \cos \tilde{\theta})}, \quad (4)$$

$$\delta_b(\tilde{\theta}) = \arctan \left[\frac{\tan(U_0 \cos \tilde{\theta})}{\cos \tilde{\theta}} \right].$$

The forward (δ_f) and backward (δ_b) scattering phases are related as $\delta_f(\tilde{\theta}) = U_0 \cos \tilde{\theta} + \delta_b(\tilde{\theta})$. Consequently, the (dimensionless) strength of the “local” scatterer in our model is characterized by a single parameter $U_0 = aV_o/\hbar v_F$.

Although one cannot talk about an angle of incidence in the 1D SWNT scattering problem, our result (4) for the transmis-

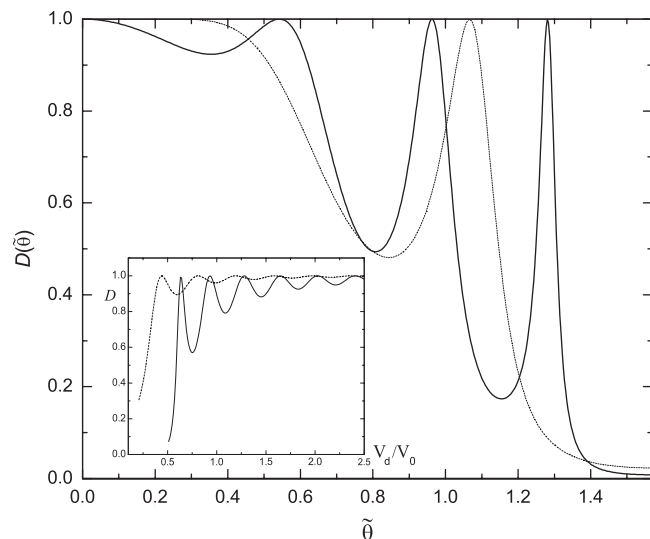


FIG. 1. Transmission coefficient as a function of chiral angle at different values of potential strength (solid curve for $U_0 = 11$ and dashed curve for $U_0 = 6.5$) and as a function of V_d/V_o (inset) at $U_0 = 8$ for different chiral angles (solid curve for $\tilde{\theta} = 0.52$ and dashed curve for $\tilde{\theta} = 0.2$).

sion coefficient D coincides—after a change of notation—with the analogous expression for the transmission coefficient in graphene.¹¹ In our case, the chiral angle $\tilde{\theta}$ formally plays the role of the angle of incidence of a particle scattered by a rectangular electrostatic barrier in graphene. It should be stressed that chiral tunneling in SWNTs differs from the phenomenon of Klein tunneling. In nanotubes, chiral tunneling is induced by the interplay of local electrostatic (scalar, V_d) and pseudomagnetic (vector, V_o) potentials, whereas in graphene, the pure electrostatic potential already leads to finite electron backscattering ($R \neq 0$) for angles of incidence $\theta \neq 0$.¹¹ In the general case $V_d \neq V_o$, the expressions (3) for the scattering data cannot be reduced to Klein tunneling in graphene. From the dependence of the transmission probability on $\tilde{\theta}$ shown in Fig. 1 for different values of the potential strength U_0 , we observe that, for a sufficiently strong ($U_0 > 1$) potential, the transmission probability is an oscillating function of the chiral angle $0 \leq \tilde{\theta} \leq \pi/2$.

From Eq. (4), one finds that $D(\tilde{\theta} = 0) = 1$ irrespective of the potential strength, which is a manifestation of the Klein paradox. In addition, one finds maxima $D(\tilde{\theta}) = 1$ for $U_0 \cos \tilde{\theta} = \pi N$, where N is an integer. The minimal value of the transmission probability, $D_{\min} = \cos^2 \tilde{\theta}$, is reached at $U_0 \cos \tilde{\theta} = \pi(N + 1/2)$. We will refer to these cases as on- and off-resonance chiral tunneling. To understand the physical meaning of these quantization conditions and the oscillations of the transmission coefficient, it is useful to consider the spectrum of the Dirac equation with a constant matrix potential given by Eq. (2). It reads $E = V_d \pm \hbar v_F \{ [p + \tilde{U}_0 \cos(\theta - \alpha)]^2 + \tilde{U}_0^2 \sin^2(\theta - \alpha) \}^{1/2}$, where $\tilde{U}_0 \equiv |V_o|/\hbar v_F$. The only effect of the uniform diagonal (electrostatic) potential V_d is a constant shift of the energy spectrum. The influence of the pseudomagnetic (off-diagonal) potential V_o is more interesting. This is because it brings about an opening of a gap, $\Delta_g = 2\hbar v_F \tilde{U}_0 \sin(\theta - \alpha)$, in the energy spectrum and plays

the role of a vector potential by shifting the momentum to $p + \tilde{U}_0 \cos(\theta - \alpha)$. We will call the quantity $\phi_c = U_0 \cos(\theta - \alpha)$ the *chiral phase* (or *chiral flux*) since it appears as an Aharonov-Bohm-like phase in chiral tunneling.

Another interesting limit of Eq. (3) is $V_d = 0$ [while for $V_o = 0$ we always have $D(\tilde{\theta}) = 1$]. In this case, the transmission probability takes the simple form $D(\tilde{\theta}) = 1/\cosh^2(U_0 \sin \tilde{\theta})$. For chiral tunneling ($\tilde{\theta} \neq 0$), the transmission probability D is smaller than unity and, in general, exponentially small for strong potentials (as in the case of ordinary tunneling). The oscillatory dependence of the transmission probability $D(\tilde{\theta})$ on the ratio V_d/V_o is presented in Fig. 1 (inset), which confirms that chiral tunneling is most pronounced when $V_o \simeq V_d$.

Next we consider the effects of chiral tunneling in two phase-coherent phenomena: the Josephson current in a nanotube-based SNS junction and the persistent current in a circular nanotube. Both systems have been studied experimentally.^{12,13}

IV. JOSEPHSON CURRENT IN A CHIRAL SNS JUNCTION

To calculate the supercurrent in the SNS junction from the relation $J = (4e/\hbar)\partial\Omega/\partial\varphi$ (where Ω is the thermodynamic potential, φ is the phase difference, and the factor 4 accounts for spin and valley degeneracies), we need to know the spectrum of Andreev bound states in the normal region [where here a SWNT containing a “soft” scatterer is characterized by Eq. (4), while the superconductor–normal metal boundaries are assumed to be fully transparent]. To this end, we follow the standard approach and solve the Bogoliubov-de Gennes (BdG) equation with a piecewise-constant magnitude $(\Delta_0, 0, \Delta_0)$ and phase of the order parameter.

In this way, we obtain the usual bound-state energies in a superconductor–normal metal–insulator–normal metal–superconductor (SNINS) junction (see, e.g., Ref. 14), where all the SWNT-specific information is included in the transmission probability $D(\tilde{\theta})$. Neither the scattering phases $\delta_{f,b}$ nor the chiral phase ϕ_c appear in the spectral equation. The scattering phases, being energy-independent quantities in our model, cancel (as in the case of an ordinary SNS junction) since they have opposite signs for electrons and holes. In the absence of backscattering ($U_0 = 0$), the nanotube chirality has no influence on the Josephson current.

In light of this, one may inquire what effect chiral tunneling could have on the Josephson current. For chiral tunneling, the junction transparency is an oscillating function of the potential strength U_0 . Therefore, one may expect a nonmonotonic behavior of the maximal supercurrent as a function of U_0 . For resonant chiral tunneling, the junction becomes fully transparent ($D_r = 1$) and the supercurrent coincides (up to a statistical factor of 2) with the Josephson current in a superconducting constriction.¹⁵ The dependence of the critical (maximal) current on U_0 is shown in Fig. 2. The junction transparency is minimal, $D_{\min} = \cos^2 \tilde{\theta}$, for off-resonance chiral tunneling. In this case, the energy gap between the Andreev levels in a junction that is short compared to the superconducting coherence length is $E_g(\tilde{\theta}) = 2\Delta_0 \sin \tilde{\theta}$, which could be very small for nanotubes with small chiral angles. If so, this would be of importance and relevant, e.g.,

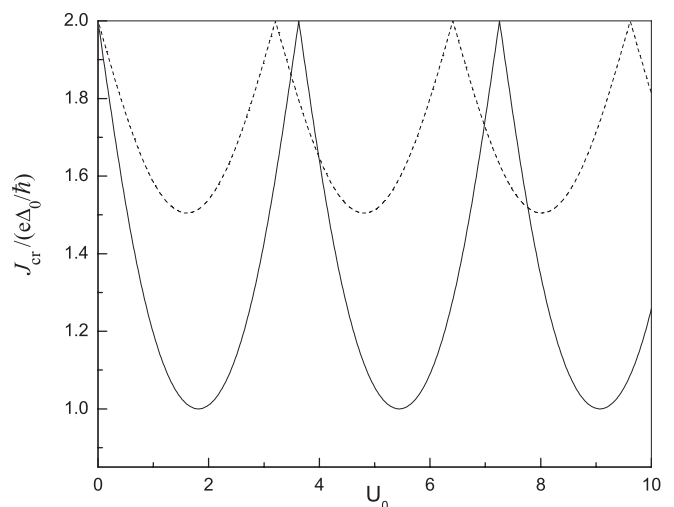


FIG. 2. The Josephson critical current (in units of $e\Delta_0/\hbar$) in a short junction as a function of the potential strength U_0 for chiral angles $\tilde{\theta} = 0.52$ (solid curve) and $\tilde{\theta} = 0.2$ (dashed curve).

for a recently proposed method for cooling the vibrations of a suspended nanotube.¹⁶

V. SPONTANEOUS PERSISTENT CURRENT

We turn next to the persistent current in a circular SWNT, where the chiral phase influences the spectrum. A local chiral scatterer, characterized by Eq. (4), is placed in a ring-shaped nanotube of circumference L , which is threaded by a magnetic flux Φ . We then consider two sets of plane-wave solutions of the Dirac equation, one to the left (l) and one to the right (r) of the scatterer. By using the Aharonov-Bohm boundary condition $\Psi_r(x + L) = \exp(2\pi i \Phi/\Phi_0) \Psi_l(x)$ (where $\Phi_0 = hc/e$ is the flux quantum) and relating Ψ_l and Ψ_r at the position of the scatterer by means of Eq. (4), one readily finds the energy spectrum to be

$$\frac{E_{n,j}L}{\hbar v_F} = \pm \arccos[\sqrt{D(\tilde{\theta})} \cos(\chi_j)] + \delta_b(\tilde{\theta}) + 2\pi n. \quad (5)$$

Here, $n = 0, \pm 1, \pm 2, \dots$; $j = \pm 1$ denotes the electron energies in the $\pm k_F$ valley; and $\chi_j = 2\pi \Phi/\Phi_0 - j\phi_{\text{eff}}$ and $\phi_{\text{eff}} = k_F L - \phi_c(\tilde{\theta})$ is the effective dimensionless flux. The term $k_F L$ represents a “statistical flux,” which results in parity effects for spinless electrons in an isolated ring (see, e.g., Ref. 17). Chiral tunneling introduces an additional term, namely, the chiral flux. Note that particles in the $\pm k_F$ valleys feel effective fluxes of opposite sign.

Evaluating the persistent current in a ring at a given chemical potential μ as $J(\Phi; \phi_c, \mu) = -c\partial\Omega/\partial\Phi$ (where Ω is the grand canonical thermodynamic potential) for the energy spectrum (5) is rather straightforward. The result at low temperatures $T \ll \hbar v_F/\pi L$ and zero chemical potential (undoped ring) is

$$J(\Phi; \phi_c) = \frac{4}{\pi} I_0 \sum_{j=\pm} \frac{\sin(\chi_j)}{\sqrt{D^{-1}(\tilde{\theta}) - \cos^2(\chi_j)}} \times \sum_{k=1}^{\infty} \frac{\sin[k \arccos[\sqrt{D(\tilde{\theta})} \cos(\chi_j)]] \cos[k\delta_b(\tilde{\theta})]}{k}, \quad (6)$$

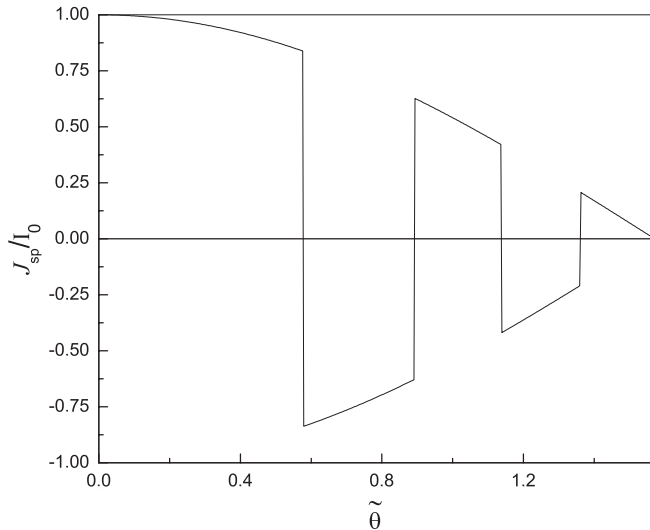


FIG. 3. Spontaneous persistent current (in units of $I_0 = ev_F/L$) as a function of chiral angle $\tilde{\theta}$ for the potential strength $U_0 = 15$.

where $I_0 = ev_F/L$. We observe from Eq. (6) that there is a *spontaneous* persistent current (i.e., at zero external magnetic flux $\Phi = 0$; see Ref. 18) in each valley ($j = \pm$). However, at equilibrium and for a ring with a fixed chemical potential (in particular $\mu = 0$), when the energy levels in the two valleys are equally populated, the net persistent current at zero flux vanishes: $J(\Phi = 0; \phi_c) = 0$.

A net spontaneous current can appear in an isolated SWNT ring with a nonequilibrium population of Dirac points. This happens for an isolated ring with an odd number of spin-1/2 fermions and in the absence of $2k_F$ backscattering. Under these conditions, there is always one “uncompensated” electron with definite spin projection and definite chirality ($\eta = \pm$) at one of the two ($j = \pm$) Dirac points. The spontaneous current,

$$J_{\text{sp}} = j\eta \frac{ev_F}{L} \frac{\sqrt{D(\tilde{\theta})} \sin(U_0 \cos \tilde{\theta})}{\sqrt{1 - D(\tilde{\theta}) \cos^2(U_0 \cos \tilde{\theta})}} = \pm I_0 \text{sgn}(\sin(U_0 \cos \tilde{\theta})) \cos \tilde{\theta}, \quad (7)$$

is associated with the partial current of this zero-energy state. Figure 3 illustrates the behavior of the spontaneous current as a function of chiral angle $\tilde{\theta}$. Note that the current abruptly

changes sign at the on-resonance points. Irrespective of the actual potential strength U_0 , the amplitude of the current corresponds to the off-resonance case $|J_{\text{sp}}| = I_0 [D_{\text{min}}(\tilde{\theta})]^{1/2} = I_0 \cos \tilde{\theta}$. This current is analogous to the semiresonance peaks in the persistent current oscillations considered in Ref. 19.

VI. CONCLUSIONS

In summary, we have extended the concept of chiral tunneling to metallic single-wall carbon nanotubes. This phenomenon, which originates from an interplay between electrostatic (V_d) and pseudomagnetic (V_o) potentials, is pronounced when $V_o \simeq V_d$. The characteristic value of V_o (caused by lattice deformations) is about 1 eV, but the same lattice deformation leads to a much larger potential V_d (of the order of 10 eV).¹⁰ Consequently, to achieve optimal chiral tunneling conditions, the electrostatic potential has to be tuned, e.g., by a local gate. Notice that the electron-electron interaction, neglected here, does not renormalize intravalley electron backscattering. This is because the resulting smooth redistribution of electron-charge density does not influence the transmission of 1D Dirac-like electrons. This assertion was explicitly verified by our calculation of the interaction-renormalized electron reflection probability for weakly interacting electrons using the model as in Ref. 20. Energy scales induced by the finite curvature of the nanotube walls (a small band-gap, spin-orbit splitting) are of the order of 10 K for nanotubes with diameter $d \simeq 1$ nm. To diminish the influence of these effects on chiral tunneling, one can use either nanotubes with larger diameter (a few nanometers) or nanotubes with small chiral angles.

ACKNOWLEDGMENTS

Discussions with L. Gorelik, A. Kadigrobov, S. Kulinich, and V. Shumeiko, as well as financial support from the Swedish VR, the EC (Grants No. FP7-ICT-2007-C and No. 225955 STELE), and the Korean WCU program funded by MEST/NFR (Grant No. R31-2008-000-10057-0), are gratefully acknowledged. The work of E.N.B. and U.L. was supported by the US Department of Energy (Grant No. FG05-86ER 45234). I.V.K. thanks the Department of Physics at the University of Gothenburg for their hospitality.

*parafilo_sand@mail.ru

¹O. Klein, *Z. Phys.* **53**, 157 (1929).

²P. L. McEuen, M. Bockrath, D. H. Cobden, Y. G. Yoon, and S. G. Louie, *Phys. Rev. Lett.* **83**, 5098 (1999).

³A. H. Castro Neto, F. Guinea, N. M. R. Peres, K. S. Novoselov, and A. K. Geim, *Rev. Mod. Phys.* **81**, 109 (2009).

⁴I. O. Kulik Pisma, *Zh. Eksp. Teor. Fiz.* **11**, 407 (1970) [*JETP Lett.* **11**, 275 (1970)].

⁵C. L. Kane, E. J. Mele, A. T. Johnson, D. E. Luzzi, B. W. Smith, D. J. Hornbaker, and A. Yazdani, *Phys. Rev. B* **66**, 235423 (2002).

⁶The chiral angle is defined as in Ref. 5 ($\theta = 0$ for an armchair nanotube and $\theta = \pi/6$ for a zigzag nanotube).

⁷C. L. Kane and E. J. Mele, *Phys. Rev. Lett.* **78**, 1932 (1997).

⁸The effective scattering potential in Eq. (2) has been derived microscopically for electron scattering in metallic carbon nanopeapods (Ref. 5).

⁹N. Levy, S. A. Burke, K. L. Meaker, M. Panlasigui, A. Zettl, F. Guinea, A. H. Castro Neto, and M. F. Crommie, *Science* **329**, 544 (2010).

¹⁰H. Suzuura and T. Ando, *Phys. Rev. B* **65**, 235412 (2002).

¹¹M. I. Katsnelson, K. S. Novoselov, and A. K. Geim, *Nature Phys.* **2**, 620 (2006).

¹²R. Martel, H. R. Shea, and Ph. Avouris, *Nature (London)* **398**, 299 (1999).

¹³A. Yu. Kasumov, R. Deblock, M. Kociak, B. Reulet, H. Bouchiat, I. I. Khodos, Yu. B. Gorbatov, V. T. Volkov, C. Journet, and M. Burghard, *Science* **284**, 1508 (1999).

- ¹⁴P. F. Bagwell, *Phys. Rev. B* **46**, 12573 (1992).
- ¹⁵I. O. Kulik and A. N. Omelyanchouk, *Fiz. Nizk. Temp.* **3**, 945 (1977) [*Sov. J. Low Temp. Phys.* **3**, 459 (1977)].
- ¹⁶G. Sonne, M. E. Pena-Aza, L. Y. Gorelik, R. I. Shekhter, and M. Jonson, *Phys. Rev. Lett.* **104**, 226802 (2010).
- ¹⁷D. Loss, *Phys. Rev. Lett.* **69**, 343 (1992).
- ¹⁸I. O. Kulik, *Fiz. Nizk. Temp.* **30**, 705 (2004) [*Low Temp. Phys.* **30**, 528 (2004)].
- ¹⁹P. Sandström and I. V. Krive, *Phys. Rev. B* **56**, 9255 (1997).
- ²⁰D. Yue, L. I. Glazman, and K. A. Matveev, *Phys. Rev. B* **49**, 1966 (1994).